J. Plasma Fusion Res. SERIES, Vol. 5 (2002) 292–296

Profiles of Divertor Plasma in Heliotron J

ANG Wanleng, MIZUUCHI Tohru[1], NAKASUGA Masahiko[1], SANO Fumimichi[1], KONDO Katsumi, NAGASAKI Kazunobu[1], OKADA Hiroyuki[1], BESSHOU Sakae, MANABE Yoshito, SHIDARA Hiroyuki, KAWAZOME Hayato, MAENO Shogo, TAKEDA Masafumi, TAKAMIYA Tasho, TOMIYAMA Keishi, TSURU Hiroki, OHNO Yoshinori, KUBO Hiroyasu, NISHIOKA Yusuke, YUKIMOTO Hidetoshi, IRIGUCHI Masao and OBIKI Tokuhiro[1]

Graduate School of Energy Science, Kyoto University, Gokasho, Uji 611-0011, Japan

[1] Institute of Advanced Energy, Kyoto University, Gokasho, Uji 611-0011, Japan

(Received: 11 December 2001 / Accepted: 5 July 2002)

Abstract

To investigate the property and structure of the diverted plasmas heated by 53.2GHz 2nd harmonic ECH in Heliotron J, two sets of Langmuir probe arrays with two dimensional spatial resolution were installed at the divertor legs which lie up-down symmetrically in the topology of the magnetic field. A clear up-down asymmetry was observed in the profiles of the density and the floating potential. The asymmetric profiles were turned over when the direction of the confinement field was reversed. As one of the candidates for the mechanism causing the asymmetry, the effect of ∇B drift on the particle transport has been investigated qualitatively and numerically by the particle orbit-guiding center tracing calculation. In the numerical results, an asymmetric profile and its reversal are observed.

Keywords:

Heliotron J, edge field structure, divertor, divertor probe array, divertor flux asymmetry, ∇B drift

1. Introduction

Handling of the heat and particle flux coming from the core plasma to the first wall is a fatal problem for fusion reactors. The concept of a divertor has been proposed as an essential and effective way to overcome this problem since the dawn of fusion research.

In the diverted tokamaks, asymmetries between the inner and outer (in-out asymmetry) divertor flux for both single-null and double-null discharges have been noticed. In addition to the in-out asymmetry, the up-down asymmetries have been observed in double-null discharges [1]. As the crucial characteristic of the asymmetry, the dependencies of the asymmetry on the direction of the confinement field have been shown [1,2]. Also, in heliotron/stellarator devices, which have intrinsic diverted field lines, the asymmetry of divertor flow and its field dependence have been observed [3,4].

Experimental and numerical studies of divertor have been performed for Heliotron J, which is a helical-axis heliotron [5] device newly constructed in Kyoto University. One of the main purposes is to find the configuration suitable for divertor in the helical-axis heliotron. Besides, it is of interest and important to ascertain if there is any asymmetry in the divertor flow as seen in other heliotron/stellarator devices and to understand the mechanism causing the asymmetry so that a scenario for the controllable divertor can be supplied. As the first step of experimental study, the standard configuration with an intrinsic helical divertor structure has been chosen and the divertor plasmas have been measured using two sets of Langmuir probe array. In this paper, the profiles of divertor plasmas, the observed asymmetry in these profiles and an ion orbit-

Corresponding author's e-mail: ang_wl@center.iae.kyoto-u.ac.jp

guiding center tracing calculation are discussed.

2. Experimental Arrangement

Heliotron J is a helical axis heliotron device with an $l = 1/m = 4$ continuous helical coil. The major radius is 1.2 m and the minor radius is 0.1–0.2 m. There are six sets of coils which can produce various configurations with various edge field structures by changing the current ratio. In the standard configuration, the whisker-structures of field lines covering the LCFS are observed [6]. A part of these whisker-structures crosses the inner wall of the device, forming four main divertor legs in one toroidal period of magnetic field (B-field), two in the high field side and others in the low field side [6,7]. Divertor legs corresponding to this configuration have localized distribution on the chamber wall and the distribution has dependence on the direction of the B-field.

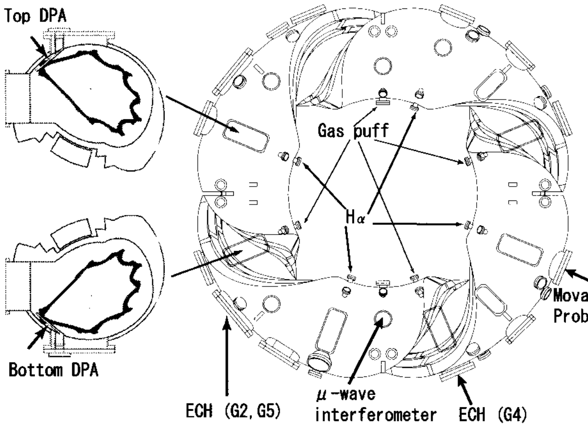

Fig. 1 Experimental set-up of heating equipments and diagnostics in the Heliotron J device.

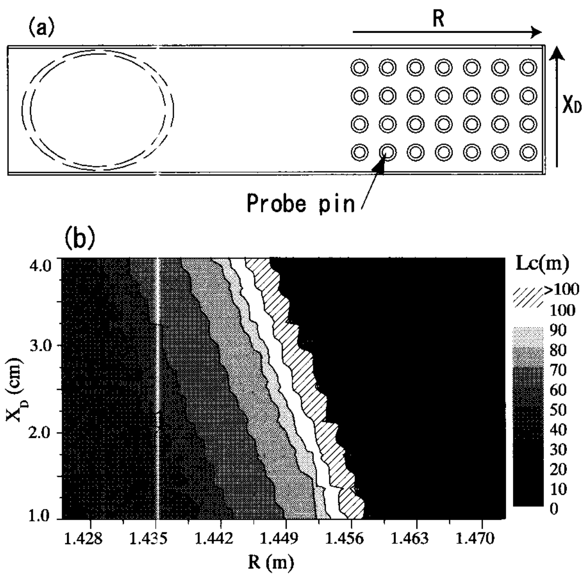

Fig. 2 (a) Arrangement of the DPA, (b) profile of connection length on the region surrounding the probe pins.

Figure 1 shows the experimental set-up of heating equipment and diagnostics in the Heliotron J device. In this study, the current-less plasmas were initiated and heated by 53.2 GHz second harmonic ECH with the maximum total power of ~400 kW from three gyrotrons (G2, G4, G5).

To investigate the property and the structure of diverted plasmas, two sets of divertor probe arrays (DPA) were installed at the up-down symmetric positions, ϕ=67.5° (top) and the ϕ=112.5° (bottom), corresponding to the low field side divertor legs in the standard configuration. The installation positions of the DPA are illustrated in Fig. 1 with the Poincare-plots of the edge field lines.

The each DPA consists of 28 dome-shaped Langmuir probes. Figure 2(a) shows a schematic of the probe pin arrangement viewing from the plasma side. The probe pins are arranged in a 4×7 matrix, in the nearly toroidal direction X_D and the nearly major radius direction R_D. Figure 2(b) shows the contour of the connection length (L_c) of the divertor field lines crossing the DPA.

3. Experimental Results

In a typical ECH discharge where the density is low ($<n_e>_{line}$~10^{19} m^{-3}, T_e~500 eV), the electron temperature T_e, the divertor plasma density n_d and the floating potential V_f deduced from the Langmuir probe I-V characteristic were found to be in the range of T_e~10–40 eV, n_d~1×10^{18}–4×10^{18} m^{-3}, V_f~-60–10 V, depending on the position of the probe tip. Figure 3 show the contour plots of T_e, n_d and V_f observed at the top and bottom DPA, respectively. As shown in this figure, the distribution of the plasma on the both DPAs seems to shift to the smaller R as increasing X_D (the dashed lines are added to the contour of maximum n_d for the sake of making a clear image). This characteristic of overall plasma distribution is basically consistent with the angle of the L_c-contours as shown in Fig. 2(b). Note that the contour of the connection length is the same for both DPAs due to the up-down symmetry of the field structure. However, quite different characteristics of the radial (R) plasma profile were observed, especially in n_d

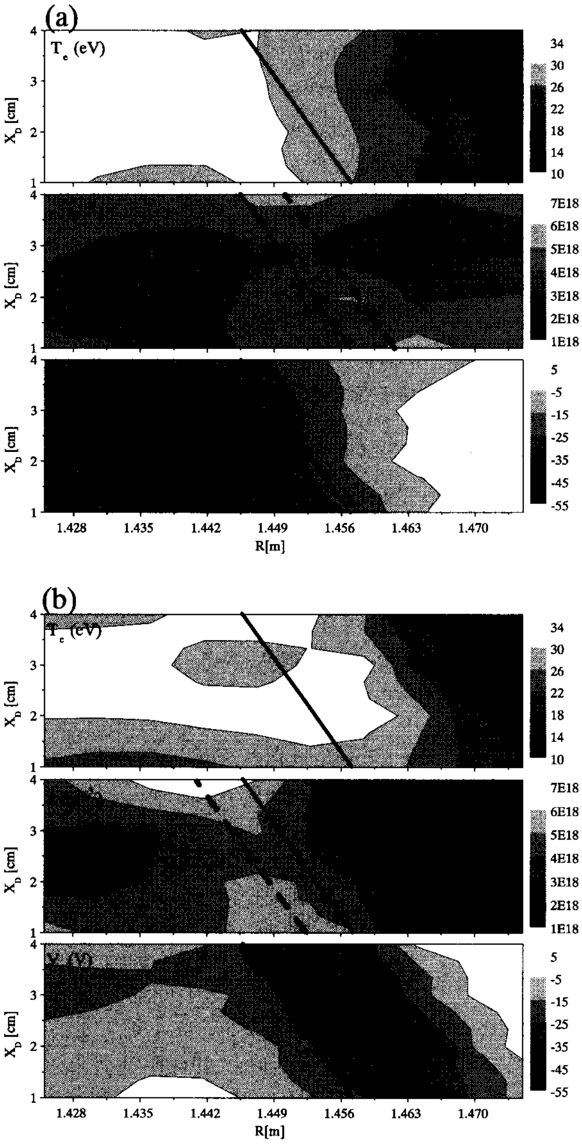

Fig. 3 Profiles of electron temperature, density and floating potential at (a) the top DPA and (b) the bottom DPA. Dashed and solid lines are added to indicate the density peaks and the approximate peak L_c contour while arrows indicate the ∇B drift direction of ions.

and V_f profiles. The peak positions of the n_d profile for the DPA differ from each other; for the top DPA it seems to be shifted to the right side (larger R side) of the peak L_c-contour while that for the bottom one is shifted to the left. Also, the V_f profiles show some distinct structures. For example, in the cross section with X_D=1 cm, as show in Fig. 4, in the top DPA, V_f has an almost constant negative value for R<1.455 m and changes to positive value for R≈1.470 m. On the other hand, in the

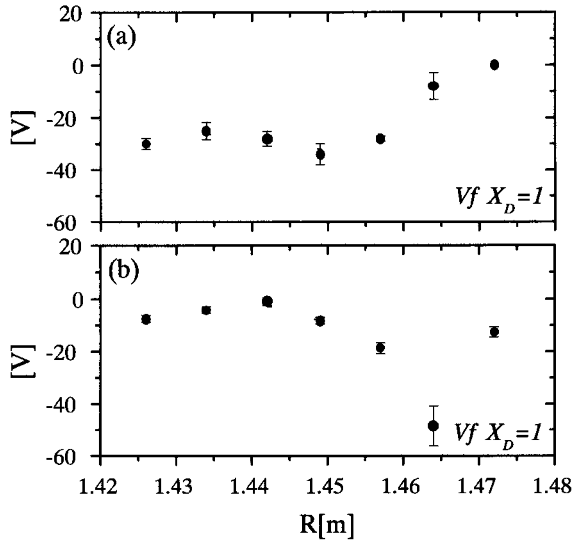

Fig. 4 Profiles of the floating potential at (a) the top DPA and (b) the bottom DPA.

bottom DPA, $V_f(R)$ is close to zero but has a sharp negative dip near R=1.465 m. These features of the divertor plasma profile observed for each DPA were completely turned over when the direction of the confinement field was reversed, the profile of top DPA as shown in Fig. 2(a) come to appear at the bottom DPA as the direction of the confinement field was reversed, vice versa.

4. Discussion

The dependence of the divertor plasma asymmetry on the direction of the confinement field assured us that this asymmetry was not a measuring error but was caused through some physical mechanism related to the magnetic field such as the ∇B drift. In order to understand this mechanism, it is necessary to consider the plasma transport not only in the edge region but also in the core region and the resulting plasma distribution on the LCFS. However, as the first step of the investigation, the ∇B effect on the particle orbit in the edge region is discussed here.

The ∇B drift direction of ions is qualitatively consistent with the observed shift of the density peaks described in the previous section, at the top DPA it points to the right side (larger R side) and at the top to the left side. The region corresponding to ∇B drift direction of ion would suffer an excess of ion flux, and the floating potential in this region can have a relatively positive value since the polarity of the local potential may be defined by the ratio of the ion to electron flux.

From these viewpoints, it can be qualitatively understood that, at the bottom DPA, the region for R<1.45 m (for X_D=1 cm), which corresponds to the ∇B drift direction of ion, has a more positive value while the region for R>1.46 m has a more negative value while the opposite is true at the top DPA. The polarity of the floating potential near the vicinity of the LCFS was negative from the measurement of the movable probe. At both DPAs, the floating potential of the regions corresponding to the SOL may be negative in the polarity. Nevertheless, a negative but more positive value (than that observed at the top one) of the floating potential at the bottom DPA for the region R<1.45m as mentioned above is supposed to be a results of the condition that more incident and hence excess of ions occurred due to the drift effect for this region.

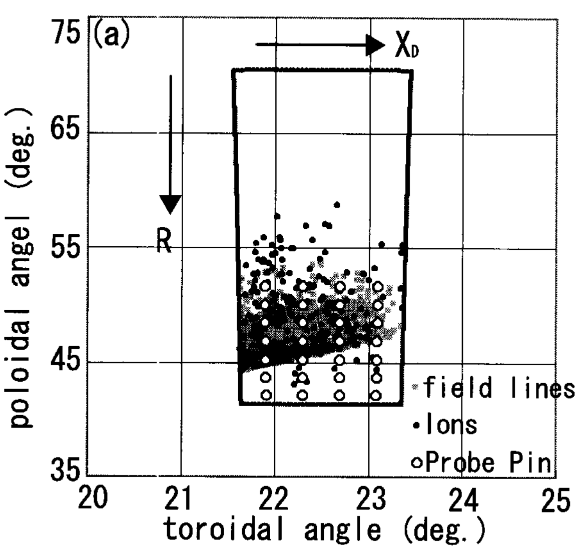

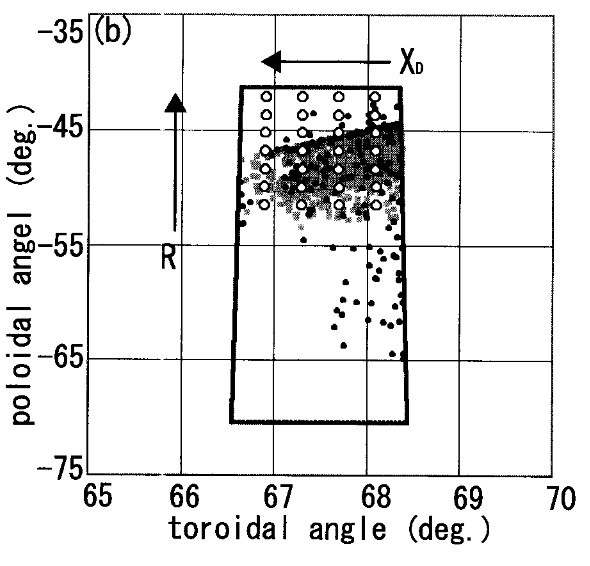

Fig. 5 Ions hitting points on the DPA surfaces corresponding to (a) the top DPA, (b) the bottom DPA. Distribution of footprint of field lines and the positions of probe pin are also shown for comparison.

The effect of the ∇B drift on the ion orbit in the edge region is investigated by using an orbit-guiding center tracing code. This calculation can reproduce an asymmetric distribution and its reversal depending on the field direction. Figure 5 shows one example of the calculated results showing the distribution of "footprint" of the ion and the field line on the DPA. Here, 10,000 ions with 20 eV energy and random pitch angles were traced starting at a random position on the LCFS (assuming an uniform plasma distribution). The ions on the bottom DPA tends to spread in the ∇B drift direction wider than that of the top DPA, forming an asymmetry between the two DPA. This is consistent with the qualitative expectation discussed above. On the other hand, the electron "footprint" is known to be similar to the symmetric distribution of footprint of field lines. The existance of different regions with excess of ion and regions with lack of ion is believed to be one of the reason for the formation of the complicated V_f profile. However, the distribution of test particles in the numerical calculation is much wider than the measuring range of existing DPAs. Therefore, a new DPA with wider measuring range is needed to make further comparison with the calculation result. Also, to obtain the correct understanding about the effect of the ∇B drift, it is necessary to carry out further experimental investigation on the distribution upstream of the diverted plasma and numerical studies on the effects of electric field and collisions.

5. Summary

The divertor plasma distribution in the standard configuration of Heliotron J has been investigated at the geometrically symmetric (up-down) positions. For ECH plasmas, the overall distribution is basically consistent with that expected from the field calculation. The detailed analysis of the n_d and V_f profiles showed, however, the existence of a clear up-down asymmetry. In order to understand this observation, the ∇B drift effect on the ion orbit in the edge region was discussed. The asymmetric spread of ion due to the ∇B effect is supposed to be account for the formation of asymmetric experimental profiles.

Acknowledgement

The authors are deeply grateful to the member of the Heliotron J group for their collaboration in the experiments and discussions. Fruitful discussions with Dr. F. Tabares (EUTATOM-CIEMAT) are also greatly acknowledged.

References

[1] X. Bonnin and W.L. Rowan, Nucl. Fusion **39**, 1009 (1999).
[2] D.N. Hill *et al.*, Fusion Technol. **21**, 1256 (1992).
[3] T. Mizuuchi *et al.*, J. Nucl. Mater. **266-269**, 1139 (1999).
[4] Y. Feng *et al.*, Plasma Phys. Control. Fusion **40**, 371 (1998).
[5] M. Wakatani *et al.*, Nucl. Fusion **40**, 569 (2000).
[6] T. Mizuuchi *et al.*, Proc. 12th Int. Stellarator Workshop (Madison, USA, 1999).
[7] T. Mizuuchi *et al.*, Proc. 10th Int. Toki Conf. (Toki, Japan, 2000).